Understanding solvent spreading for Langmuir deposition of nanomaterial films: a Hansen solubility parameter approach

Article (Accepted Version)

Understanding solvent spreading for Langmuir deposition of nanomaterial films: A Hansen solubility parameter approach

Matthew J. Large,* Sean P. Ogilvie, Alice A. K. King, and Alan B. Dalton*

University of Sussex, Falmer, Brighton, BN1 9RH, United Kingdom

E-mail: m.large@sussex.ac.uk; a.b.dalton@sussex.ac.uk

Abstract

In order to prepare high-quality Langmuir films of two-dimensional materials it is important to select a solvent optimized for both exfoliation and spreading at the air-water interface. Whilst it is generally accepted that exfoliation and stabilisation of two-dimensional materials is well-described using the Hansen solubility parameter theory, a complementary description of solvent spreading behaviour is lacking.

To this end we develop an understanding of solvent spreading using a Hansen solubility parameter framework. Our model accurately predicts the behaviour of both water-immiscible and water-miscible solvents in Langmuir film formation experiments. We demonstrate that spreading behaviour can be modified by controlling the surface pressure of the subphase using an amphiphilic species and accordingly utilise this approach to determine the maximum spreading pressure for a selection of solvents.

Ultimately, by building on this understanding we open up additional routes to optimize the preparation of Langmuir films of two-dimensional materials and other nanoparticles.

Keywords: Langmuir film, spreading solvent, interfacial interaction

Introduction

Langmuir film formation (combined with Blodgett or Schaefer deposition methods) has emerged as an attractive method for preparation of large-area, particulate monolayer films of liquid-exfoliated graphene[1–4] and other two-dimensional (2D) nanomaterials. These structures have applications in functional coatings and thin-film electronics.

Generally, the Langmuir film preparation process involves spreading of a solvent-borne dispersion of nanoparticles over a liquid subphase (often water). Provided the solvent is of sufficiently low boiling point, it will evaporate leaving a film of isolated particles trapped at the air-subphase interface. Conventional spreading solvents, such as chloroform, are demonstrably poor exfoliating solvents for 2D materials due to high mismatches of both surface tension (affecting exfoliation efficiency[5]) and solubility parameters (affecting stability and attainable concentrations[6]). Conventional spreading solvents tend to have low boiling points and be water-immiscible. Moreover, powerful exfoliating solvents, such as *N*-methyl-2-pyrrolidone (NMP), tend to be water-miscible and have high boiling points.[6] As a result a number of recent reports turn to less orthodox Langmuir approaches, such as spreading films from NMP dispersions[4,7] (this relies on dissolution of the solvent in the subphase, rather than evaporation). Attempts have also been made to use low-concentration acetone dispersions of graphene.[8] Alternatively, dilution of NMP with chloroform has been used to tailor the vapour pressure, boiling point, and concentration of the spreading dispersion.[1] Finally, electrospraying has also been used as a method for delivering droplets of solvent dispersions onto the subphase with high efficiency.[9] For nanomaterials such as graphene oxide which have both hydrophillic and hydrophobic character, akin to amphiphilic molecules, studies of interfacial assembly have shown that pH control is also required to promote proper film formation.[10,11] All approaches aim to achieve and deposit nanomaterial dispersions with sufficient stability and material quality for preparation of high-quality and high coverage Langmuir films, with minimal material loss into the subphase.

The influence of the spreading solvent used on monolayer properties has been previously

acknowledged.[12,13] In order to make an informed selection of solvent system for preparation and deposition of nanomaterial films, it is crucial to understand the spreading behaviour of the candidate solvents. In this paper we develop a model for understanding this behaviour in terms of the Hansen solubility parameter theory. This understanding may be coupled with existing work on the exfoliation of nanomaterials in order to achieve optimized conditions for Langmuir film formation.

Results and Discussion

In order for a solvent to be used for Langmuir deposition on water, there are two conditions which should be met. Firstly, in the particular case of water-miscible solvents,[3,8] the solvent droplets should be buoyant in the subphase such that they do not sink and dissolve. Secondly, the solvent should spread on the surface of water. The former condition applies primarily to experiments where one wishes to inject dispersions beneath the air-water interface[14] (as might be done in automated experiments). The latter condition is necessary in all cases to maximise the area over which nanoparticles are spread in order to minimise reaggregation during solvent evapouration.

Figure 1 shows simple schematic geometries for treating both solvent buoyancy (Figure 1**a**) and spreading (Figure 1**b**). By evaluating the Reynolds and Peclet numbers[15] for the scenario in Figure 1**a** (using characteristic values), we find that most water-miscible solvents are sufficiently buoyant to avoid dissolution in the subphase. This is due to the low diffusivity of solvent molecules in water, relative to the velocity of the droplet under the buoyancy force. Calculations are presented in the Supplementary Information.

Examining Figure 1**b** we suggest that a basic threshold for spreading of the solvent droplet is that the equilibrium contact angle be less than 90°. This is equivalent to requiring the interfacial tension between the solvent (A) and water (B) be less than the surface tension of water; $\gamma_{AB} < \gamma_B$. Using simple continuum models to evaluate the interfacial tension in this

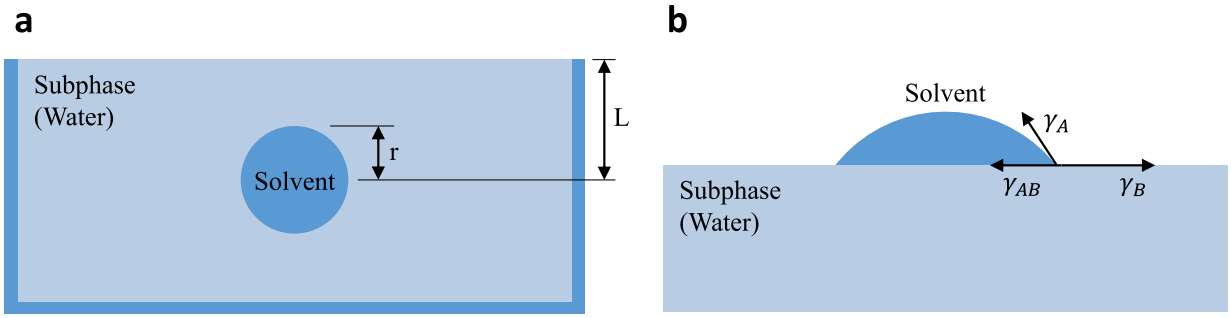

Figure 1: **a**: Schematic illustrating the buoyancy problem. A droplet of solvent with radius r is submerged at depth L in the subphase (water). **b**: Schematic illustrating the spreading problem as a spherical cap of solvent on a planar water surface. The surface tension components between solvent A and water B are labelled.

case is not instructive. This is because these models evaluate the work of adhesion using a mean of the surface tensions of the two phases; variously the geometric or harmonic means;[16]

$$\gamma_{AB} = \gamma_A + \gamma_B - 2\sqrt{\gamma_A \gamma_B}, \tag{1}$$

$$\gamma_{AB} = \gamma_A + \gamma_B - 4\frac{\gamma_A \gamma_B}{\gamma_A + \gamma_B}. \tag{2}$$

By well-known inequalities, it can be readily seen that these models necessarily yield interfacial tensions that are less than, or equal to, the larger of the two surface tensions in the system. The result of this is that the models predict that all liquids with a surface tension below that of water will spread. However, there are low surface tension liquids that contradict this predication. For example, toluene and dichloromethane both have very similar surface tensions ($\gamma = 27.8\,\mathrm{mN\,m^{-1}}$ and $\gamma = 27.9\,\mathrm{mN\,m^{-1}}$, respectively) yet the latter spreads on water and the former does not, with the main difference being that dichloromethane is a marginally more polar molecule. Evidently, we require a model which is capable of dealing with the component intermolecular interactions at the liquid-liquid interface.

Hansen solubility parameter theory[17,18] was developed as a framework for interpreting intermolecular force components in terms of their contributions to the cohesive energy of materials and their solutions. The three parameters, δ_d, δ_p and δ_h, represent contributions to

the cohesive energy density E_0 of a material due to dispersive, polar and hydrogen bonding intermolecular interactions, respectively. Their origin is in an analogy to the Hildebrand solubility parameter $\delta = \sqrt{E_0}$, and as a result the Hildebrand and Hansen parameters are related;[18]

$$E_0 = \delta^2 = \delta_d^2 + \delta_p^2 + \delta_h^2 \tag{3}$$

The solubility of a molecule A in a solvent B in the Hansen formalism is correlated with an "interaction distance" R_A between their respective sets of Hansen parameters;

$$R_A^2 = 4(\delta_d^{(A)} - \delta_d^{(B)})^2 + (\delta_p^{(A)} - \delta_p^{(B)})^2 + (\delta_h^{(A)} - \delta_h^{(B)})^2. \tag{4}$$

The quantity R_A^2 is related to the Flory-Huggins parameter χ, and so minimisation of R_A is equivalent to minimising the free energy penalty for substituting a molecule of B with one of A. In this manner solvents with a low R_A relative to a chosen material will act as "good solvents".

Table 1 shows data for a selection of solvents categorised as water-miscible and water-immiscible (a comprehensive list of investigated solvents is included in the Supplementary Information). Some solvents included are typically used for exfoliation of nanomaterials or Langmuir film formation, and others are included to cover a wide range of accessible surface tensions for the solvent phase. We see that, contrary to the predictions of the simple interfacial tension models (Equations (1) and (2)), some (but not all) of the low surface tension liquids do not spread. We note that this is not directly related to the surface tension, but that these are all non-polar (or weakly polar) liquids.

In order to understand how the Hansen parameters are linked to interfacial tension, we first look at their relationship to surface tension of a single phase. Koenhen and Smolders report a model relating these quantities to the molar volume V_M, based on the surface tension of hard sphere liquids.[19]

$$\delta_d^2 + a\delta_p^2 + b\delta_h^2 = \mathcal{A}\left(\frac{1}{V_M}\right)^{\frac{1}{3}}\gamma, \tag{5}$$

Table 1: Values of surface tension, Hansen Solubility Parameters (from Table 10.1 of Hansen's reference text[18]), and spreading behaviour for a selection of solvents.

Solvent		γ_s /mN m^{-1}	δ_d /MPa$^{1/2}$	δ_p /MPa$^{1/2}$	δ_h /MPa$^{1/2}$	Spreads?
Miscible	Ethanol	22.0	15.8	8.8	19.4	Y
	Acetone	23.0	15.5	10.4	7.0	Y
	Isopropanol	23.3	15.8	6.1	16.4	Y
	N-methyl-2-pyrrolidone	40.8	18.0	12.3	7.2	Y
Immiscible	Hexane	18.8	14.9	0.0	0.0	N
	Chloroform	26.7	17.8	3.1	5.7	Y
	Dichloromethane	27.8	18.2	6.3	6.1	Y
	Toluene	27.9	18.0	1.4	2.0	N
	Cyclopentanone	34.2	17.9	11.9	5.2	Y

where $\mathcal{A} = 0.14\,\mathrm{mol}^{-1}$; the constants a and b take different values for alcohols ($a = 1$, $b = 0.06$) and non-alcohols ($a = b = 0.63$), based on a solvent database fitting analysis.[19]

Koenhen and Smolders' model utilises the Hansen parameters to estimate the deviation in cohesive energy density at the liquid surface; and hence estimate the surface tension. This explains the similarity of the left hand side of Equation (5) to the right hand side of Equation (3). By analogy to Equation (4), and substituting the molar volume for an average value $V_M \to 0.5(V_M^{(A)} + V_M^{(B)})$, we suggest that the cohesive energy density deviation at an interface (and thus the interfacial tension) can be approximated;

$$\begin{aligned}(\delta_d^{(A)} - \delta_d^{(B)})^2 + (\sqrt{a^{(A)}}\delta_p^{(A)} - \sqrt{a^{(B)}}\delta_p^{(B)})^2 \\ +(\sqrt{b^{(A)}}\delta_h^{(A)} - \sqrt{b^{(B)}}\delta_h^{(B)})^2 = \mathcal{A}\left(\frac{2}{V_M^{(A)} + V_M^{(B)}}\right)^{\frac{1}{3}}\gamma_{AB}.\end{aligned} \tag{6}$$

Figure 2 compares the interfacial tension predictions of Equation (6) for a range of solvents to those of the models of Equations (1) and (2). In order to maintain internal consistency, the values for the surface tension in each case are those calculated using Equation (5). The shaded region identifies solvents which are predicted to not spread ($\gamma_{AB} > \gamma_B$, where B is the water subphase). For each solvent shown, the behaviour has been verified experimentally. We find that the model presented correctly identifies the behaviour of all 21

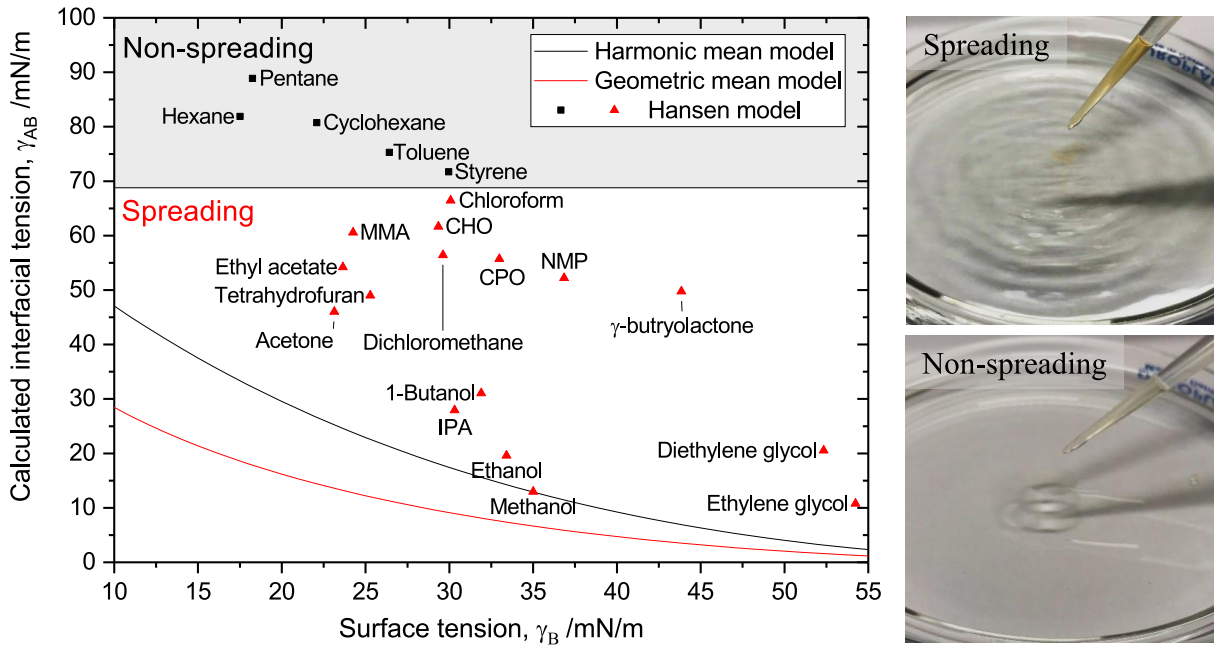

Figure 2: Calculated solvent-water interfacial tensions against surface tension of the solvent. The horizontal line represents the threshold for spreading; solvents with lower interfacial tension spread, and those with higher tension do not spread. The points represent predictions of Equation (6), and are identified as spreading (▲) and not spreading (■) according to experimental measurements. The right photographs illustrate the experimental verification of spreading (top) and non-spreading (bottom) liquids.

solvents tested for their interactions with a pristine water surface.

We note that chloroform, the prototypical spreading solvent for Langmuir experiments, falls remarkably close to the threshold value for spreading. Other solvents which have been used for spreading nanomaterial films in the literature, such as NMP and acetone, fall further from the threshold. This means that the behaviour of different solvents will be affected differently by variations in the surface tension of the water subphase. Such variations could be induced by the presence of a surface film, for example. In the simplest incarnation, we may consider a film of amphiphillic molecules present at the air-water interface, which leads to a measurable surface pressure Π. Figure 3**a** shows a modification to the conceptual system of Figure 1**b**. In typical Lanmguir film preparations it is assumed that Marangoni flow drives the molecular film away from the droplet as it is brought into contact with the water surface. In this way only the *surface* tension of the subphase is modified (the *interfacial*

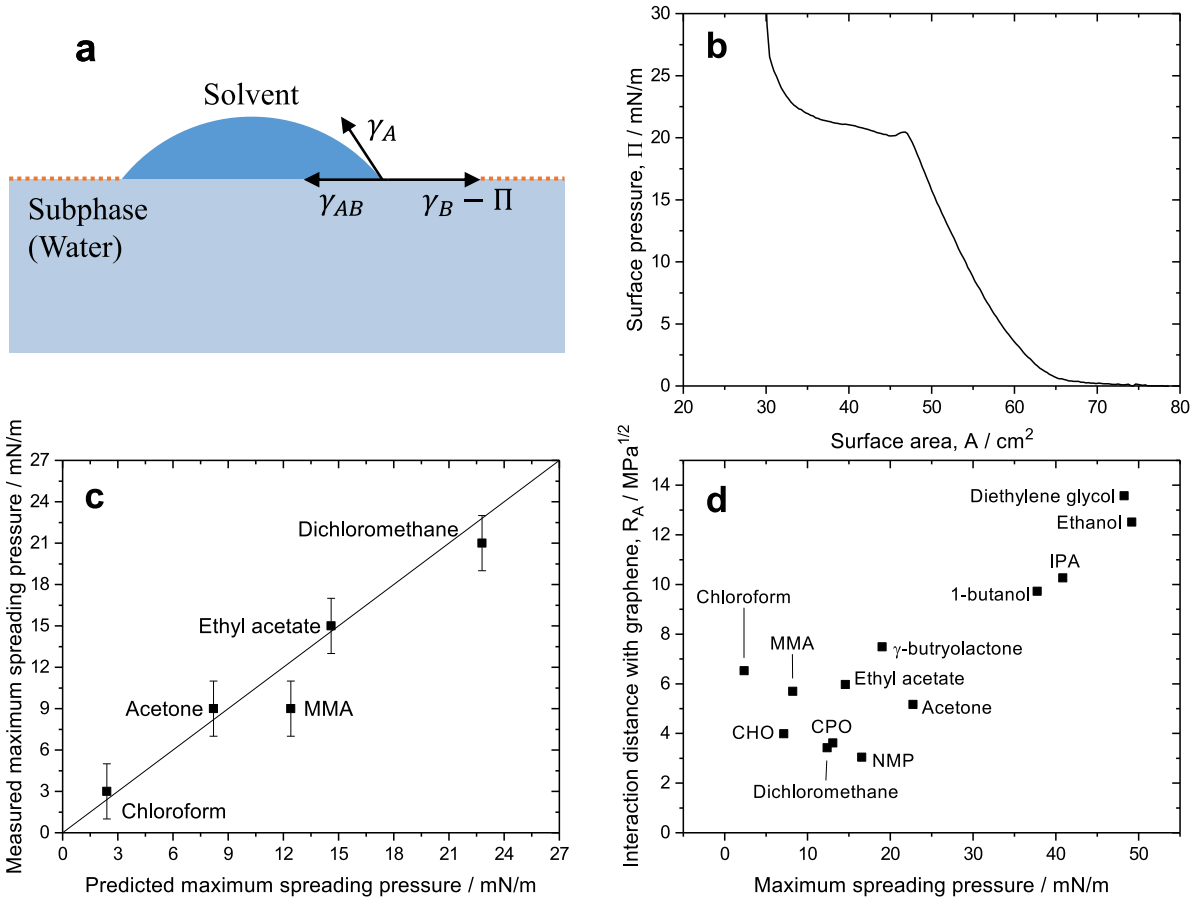

Figure 3: **a**: Modification to Figure 1**b** to account for the presence of a Langmuir film at the air-water interface. **b**: Experimental pressure-area isotherm data for arachidic acid. **c**: Experimental verification of maximum spreading pressures for some solvents. The plotted line represents $y = x$, which well represents the trend in the data. **d**: A plot of Hansen interaction distance, R_A, with graphene against predicted maximum spreading pressure.

tension γ_{AB} remains unmodified); $\gamma_A \rightarrow \gamma_A - \Pi$. As such, the effect of an increase in surface pressure will be to lower the threshold for spreading in Figure 2. Therefore the absolute difference of the predicted interfacial tension and the surface tension of water represents a threshold surface pressure above which each solvent should cease to spread in an isothermal experiment; $\Pi_{\text{max}} = \gamma_A - \gamma_{AB}$.

In order to test this facet of the model, we use a film of arachidic acid as a means to control the surface pressure. Figure 3**b** plots the pressure-area isotherm of the film. The surface pressure was gradually increased to determine the point at which five solvents

ceased to spread; the results are plotted in Figure 3**c** (a table of observations is given in the Supplementary Information). As the surface pressure is increased we observe a transition region where the solvent spreading is hindered, before the solvent droplets cease to spread and remain as biconvex droplets (with a markedly decreased evaporation rate). We define the threshold spreading pressure as the highest surface pressure where no influence on the solvent spreading is observed. Based on Figure 3**c**, we note that the data are very well represented by the line $y = x$. This strongly indicates that the model presented accurately reflects the fundamental chemical physics which drives solvent spreading on the surface of water, even in the presence of a surface-active film.

It was noted during the experiments that once the droplets ceased to spread (and therefore remained at the air-water interface for a significant length of time) an apparently crystalline film of the amphiphilic material, visible to the naked eye, formed at the solvent-water interface inside the droplet. This is due to the fact that there is some solubility of the film material in the solvent. We anticipate that this effect will influence the precise measurement of the maximum spreading pressure for each solvent, as our initial assumption was that the solvent-water interface was unmodified by the presence of the film. Also, the effective surface pressure surrounding the droplet will be lowered as the film partially dissolves in the solvent. We do however note that there is not an observable effect within the uncertainty of our existing measurements.

In a qualitative illustration of the maximum spreading pressure effect on deposition dynamics, a film of water-insoluble fluorescent material (m-phenylenevinylene trimer) was deposited from chloroform in two successive steps. High-speed camera footage (300fps) under laser illumination at 405 nm is available in the Supplementary Information. The first solvent droplet spreads and evaporates rapidly (< 2 s), but the second droplet is hindered by the presence of the material film, and so spreads and dissipates over a significantly longer time scale (~ 10 s, breaking up into several biconvex droplets in the process).

Given the success of the present model in describing pristine solvent behaviour, we seek

to incorporate existing understanding of nanomaterial-solvent interactions to optimize the solvent system for preparation of nanomaterial films. The Hansen solubility parameters have recently emerged as a powerful tool for evaluating interactions between solvents and nanomaterials, such as carbon nanotubes,[20] graphene[6,21] and other 2D nanomaterials.[22] Figure 3**d** plots the predicted maximum spreading pressure from the present model alongside the Hansen interaction distance (defined by Equation (4)) of each solvent with graphene, as an archetypal 2D nanomaterial. This latter parameter is of great importance to the solvent selection problem, since it not only relates to the maximum stable concentration of a nanomaterial dispersion (by the Flory-Huggins theory[6]), but according to Equation 6 will also correlate with the interfacial tension between an exfoliating solvent and nanomaterial. This affects the degree of exfoliation and particle size achievable in most exfoliation processes, as well as influencing the stability of obtained dispersions.

When selecting a solvent for Langmuir film preparation of 2D materials, in principle one wishes to have the minimum interaction distance with the material, as well as a solvent which spreads effectively on water. The higher the value of Π_{max} for a given solvent, the higher the achievable surface coverage without the use of compression. This is important, since the compression ratios achievable using typical Langmuir troughs is less than 10; this means to achieve complete surface coverage at full compression an initial coverage of at least 10 % is necessary. Figure 3**d** suggests that cyclohexanone, cyclopentanone, dichloromethane and NMP are the best candidate solvents (of those investigated here). Application of this understanding to the selection of a specific solvent will be affected by further considerations, such as the spreading *dynamics* (affected by solvent boiling point, viscosity) and exfoliation efficiency (surface tension mismatch) of each solvent.

Conclusions

By including information on the component interactions between molecules, we have developed an interfacial tension model capable of accurately predicting the spreading behaviour of solvents used for Langmuir experiments, even in the presence of a surface-active film.

The use of Hansen solubility parameters in the present model facilitates coupling of nanomaterial exfoliation considerations directly into the solvent selection problem. We believe this will allow for optimization of L-S and L-B-deposited nanomaterial films by minimising the number of processing steps and solvent transfers required to achieve suitable dispersions for spreading.

Materials and Methods

Materials

All solvents were purchased from Sigma Aldrich (reagent grade, $> 99\,\%$ purity) and used as-received. Ultrapure water ($18.2\,\mathrm{M\Omega\,cm}$ resistivity) was freshly prepared using a Thermo Scientific Barnstead MicroPure purification system.

Methods

A NIMA 102A Langmuir trough equipped with a platinum Wilhelmy plate was used for all experiments. The spreading behaviour of each solvent studied was established by adding a $5\,\mu\mathrm{L}$ droplet from a micropipette onto a pristine water surface. Spreading solvents rapidly spread out over the surface and evapourate within several seconds under ambient conditions. Non-spreading solvents pool into one or more droplets and evapourate at a significantly slower rate, even for comparable boiling points to spreading solvents.

To prepare a monolayer film, arachidic acid was dissolved into chloroform at $\sim 1\,\mathrm{mg\,mL^{-1}}$ concentration. $10\,\mu\mathrm{L}$ of the solution was spread onto the surface of the Langmuir trough

(74 cm^2 open area); an initial molecular density of approximately 30 $Å^2$/molecule was obtained. The isotherm of Figure 3**b** was obtained by closing the barriers at a rate of 10 $cm^2\,min^{-1}$ with a target surface pressure of 30 $mN\,m^{-1}$. To measure the maximum spreading pressure of each solvent, the barriers were initially fully opened. The surface pressure was controlled in increments of 3 $mN\,m^{-1}$, and at each increment a 5 µL droplet of pristine solvent was added to the surface for observation. Each solvent was tested separately, with the trough water and arachidic acid film replaced in between solvent tests.

Acknowlegments

The authors graciously acknowledge strategic development funding from the University of Sussex. The authors would also like to graciously thank Jayne Rowlands and Flavio Ferrari for their assistance with high-speed video capture.

Author contributions

Experimental concepts were devised by MJL and SPO. Experiments were carried out by MJL, SPO, AAKK. MJL prepared the manuscript with the assistance of SPO, ABD. AAKK and ABD reviewed the manuscript prior to submission.

References

(1) Fahimi, A.; Jurewicz, I.; Smith, R. J.; Sharrock, C. S.; Bradley, D. A.; Henley, S. J.; Coleman, J. N.; Dalton, A. B. Density Controlled Conductivity of Pristine Graphene Films. *Carbon* **2013**, *64*, 435–443.

(2) Gengler, R. Y. N.; Veligura, A.; Enotiadis, A.; Diamanti, E. K.; Gournis, D.; Józsa, C.; van Wees, B. J.; Rudolf, P. Large-Yield Preparation of High-Electronic-Quality Graphene by a Langmuir–Schaefer Approach. *Small* **2010**, *6*, 35–39.

(3) Kim, H.; Mattevi, C.; Kim, H. J.; Mittal, A.; Mkhoyan, K. A.; Riman, R. E.; Chhowalla, M. Optoelectronic Properties of Graphene Thin Films Deposited by a Langmuir–Blodgett Assembly. *Nanoscale* **2013**, *5*, 12365–12374.

(4) Matković, A.; Milošević, I.; Milićević, M.; Tomašević-Ilić, T.; Pešić, J.; Milenko Musić,; Spasenović, M.; Jovanović, D.; Vasić, B.; Deeks, C.; Radmila Panajotović,; Belić, M. R.; Gajić, R. Enhanced Sheet Conductivity of Langmuir–Blodgett Assembled Graphene Thin Films by Chemical Doping. *2D Materials* **2016**, *3*, 015002.

(5) Paton, K. R. et al. Scalable Production of Large Quantities of Defect-Free Few-Layer Graphene by Shear Exfoliation in Liquids. *Nature Materials* **2014**, *13*, 624–630.

(6) Hernandez, Y.; Lotya, M.; Rickard, D.; Bergin, S. D.; Coleman, J. N. Measurement of Multicomponent Solubility Parameters for Graphene Facilitates Solvent Discovery. *Langmuir* **2010**, *26*, 3208–3213.

(7) Li, X.; Zhang, G.; Bai, X.; Sun, X.; Wang, X.; Wang, E.; Dai, H. Highly Conducting Graphene Sheets and Langmuir–Blodgett Films. *Nature Nanotechnology* **2008**, *3*, 538–542.

(8) Large, M. J.; Ogilvie, S. P.; Alomairy, S.; Vöckerodt, T.; Myles, D.; Cann, M.; Chan, H.; Jurewicz, I.; King, A. A. K.; Dalton, A. B. Selective Mechanical Transfer Deposition of Langmuir Graphene Films for High-Performance Silver Nanowire Hybrid Electrodes. *Langmuir* **2017**,

(9) Nie, H.-L.; Dou, X.; Tang, Z.; Jang, H. D.; Huang, J. High-Yield Spreading of Water-Miscible Solvents on Water for Langmuir–Blodgett Assembly. *Journal of the American Chemical Society* **2015**, *137*, 10683–10688.

(10) Kim, J.; Cote, L. J.; Kim, F.; Yuan, W.; Shull, K. R.; Huang, J. Graphene Oxide Sheets at Interfaces. *132*, 8180–8186.

(11) Kostiuk, D.; Bodik, M.; Siffalovic, P.; Jergel, M.; Halahovets, Y.; Hodas, M.; Pelletta, M.; Pelach, M.; Hulman, M.; Spitalsky, Z.; Omastova, M.; Majkova, E. Reliable determination of the few-layer graphene oxide thickness using Raman spectroscopy. *47*, 391–394.

(12) Walker, D. C.; Jun, H. E. R. Effect of the Spreading Solvent on Monolayer Properties. *Nature* **1964**, *203*, 203292a0.

(13) Gericke, A.; Simon-Kutscher, J.; Huehnerfuss, H. Influence of the Spreading Solvent on the Properties of Monolayers at the Air/Water Interface. *Langmuir* **1993**, *9*, 2119–2127.

(14) Kaur, H.; Yadav, S.; Srivastava, A. K.; Singh, N.; Schneider, J. J.; Sinha, O. P.; Agrawal, V. V.; Srivastava, R. Large Area Fabrication of Semiconducting Phosphorene by Langmuir-Blodgett Assembly. *Scientific Reports* **2016**, *6*, srep34095.

(15) Rieutord, M. *Fluid Dynamics: An Introduction*; Springer, 2014.

(16) Wu, S. Calculation of Interfacial Tension in Polymer Systems. *Journal of Polymer Science Part C: Polymer Symposia* **1971**, *34*, 19–30.

(17) Hansen, C. The Three Dimensional Solubility Parameter and Solvent Diffusion Coefficient. *Journal of Paint Technology* **1967**, *39*, 104.

(18) Hansen, C. M. *Hansen Solubility Parameters: A User's Handbook, Second Edition*; CRC Press, 2007.

(19) Koenhen, D. M.; Smolders, C. A. The Determination of Solubility Parameters of Solvents and Polymers by Means of Correlations with Other Physical Quantities. *Journal of Applied Polymer Science* **1975**, *19*, 1163–1179.

(20) Bergin, S. D.; Sun, Z.; Rickard, D.; Streich, P. V.; Hamilton, J. P.; Coleman, J. N. Multicomponent Solubility Parameters for Single-Walled Carbon Nanotube-Solvent Mixtures. *ACS Nano* **2009**, *3*, 2340–2350.

(21) O'Neill, A.; Khan, U.; Nirmalraj, P. N.; Boland, J.; Coleman, J. N. Graphene Dispersion and Exfoliation in Low Boiling Point Solvents. *The Journal of Physical Chemistry C* **2011**, *115*, 5422–5428.

(22) Coleman, J. N. et al. Two-Dimensional Nanosheets Produced by Liquid Exfoliation of Layered Materials. *Science* **2011**, *331*, 568–571.

Graphical TOC Entry